Mahuzier et al., http://www.jcb.org/cgi/content/full/jcb.201111009/DC1

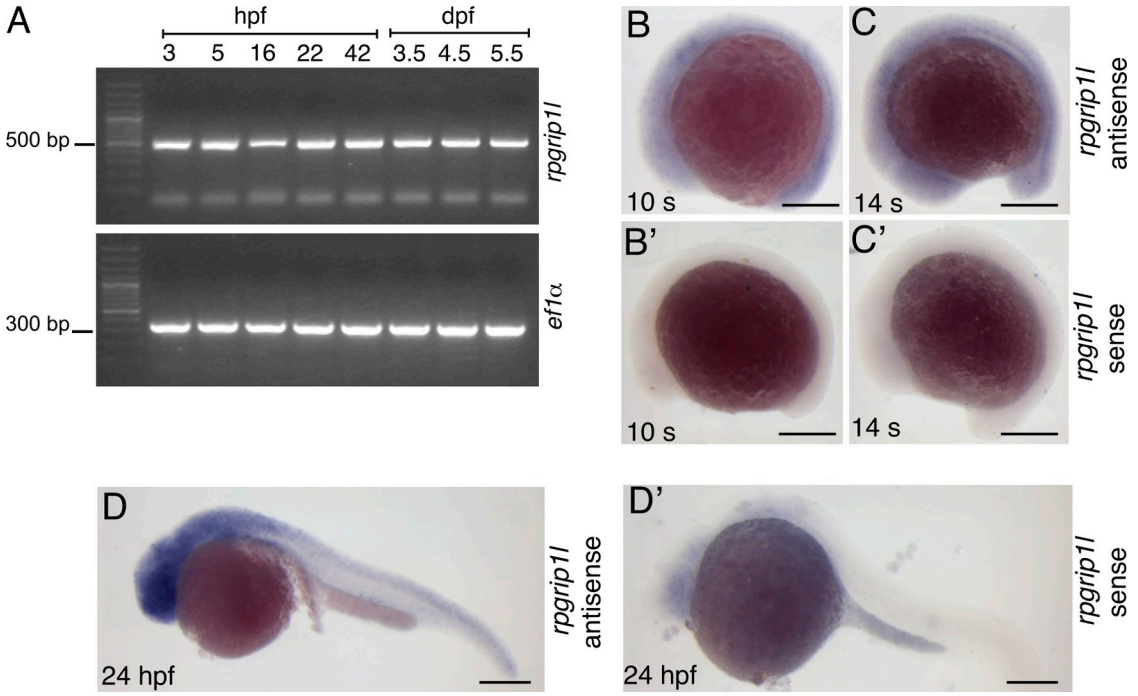


Figure S1. **Zebrafish *rpgrip1l* gene expression.** (A) RT-PCR analysis of *rpgrip1l* expression in zebrafish embryos at different stages post-fertilization. (B–D′) In situ hybridization with *rpgrip1l* antisense (B, C, and D) or sense (B′, C′, and D′) probes at the 10-s (14 hpf; B and B′), 14-s (16 hpf; C and C′), and 24-hpf (D and D′) stages. *Rpgrip1l* is expressed widely and weakly in 10-s and 14-s stage embryos, and at higher levels in the otic vesicle, the floor plate and the notochord. At 24 hpf, *rpgrip1l* is enriched in the central nervous system. Methods: RT-PCR analysis of *rpgrip1l* was performed in standard conditions, using forward (5′-GCTTTTAAATCGACTAAACGATG-3′) and reverse (5′- TGCCTGAGAGCTGCTTTCG-3′) primers. Control PCR primers for zebrafish *ef1α* were: *ef1α*-forward (5′-CTTCTCAGGCTGACTGTGC-3′) and *ef1α*-reverse (5′-CCGCTAGCATTACCCTCC-3′). For in situ hybridization, probes spanning two regions of the *rpgrip1l* cDNA, nucleotides 1004–2480 and 2348–4020, gave similar results. Bars, 250 mm. bp, base pairs.

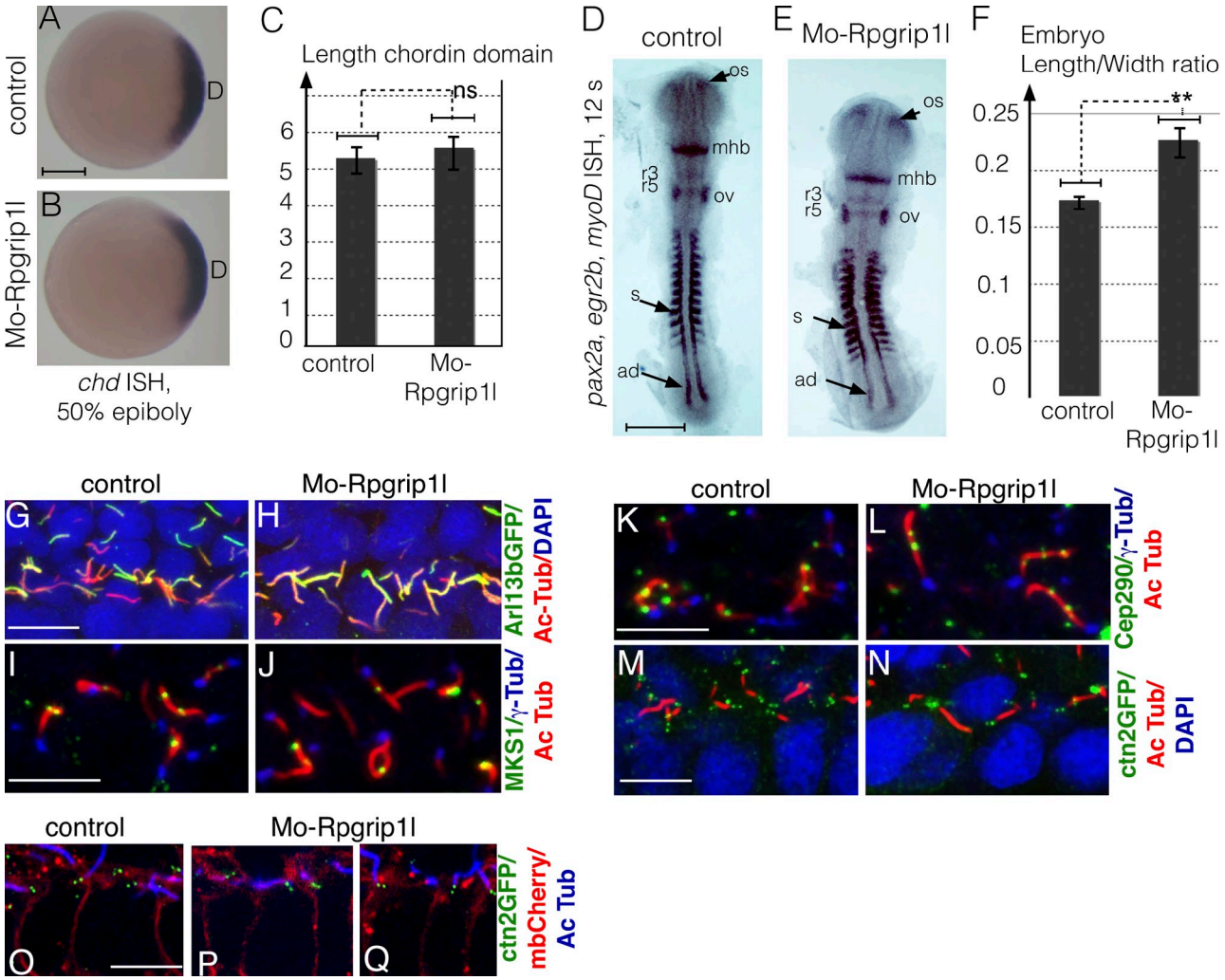


Figure S2. **No apparent defect in dorso-ventral (DV) and antero-posterior (AP) patterning, and in cilium and basal body integrity, in *rpgrip1l* morphants.** (A and B) Animal views of noninjected control (A) or Mo-Rpgrip1l–injected (B) embryos at the 50% epiboly stage after in situ hybridization (ISH) with a *chordin* (*chd*) probe. (C) Diagram illustrating the mean length of the *chd* domain (portion of the embryo perimeter presenting *chd* expression; arbitrary units) in control and Mo-Rpgrip1l–injected embryos. 5 control embryos and 17 Mo-Rpgrip1l–injected embryos were measured. No significant difference in length was found (Student's t-test, $\alpha > 0.1$; ns, non significant). *Chd* is expressed in a dorsal mesodermal domain of similar size and shape in controls and *rpgrip1l* morphants, showing that early dorso-ventral patterning is normal. (D and E) Dorsal views of flat-mounted noninjected control (D) or Mo-Rpgrip1l–injected (E) embryos at the 12-s stage after in situ hybridization with *krox20/egr2b*, *pax2a*, and *myoD* probes. *Krox20* is expressed in two hindbrain transverse domains, r3 and r5; *pax2a* expression marks the midbrain–hindbrain boundary and the optic stalk, and *myoD* is expressed in the somites and adaxial cells. Together, these three gene expression patterns provide landmarks to assess CE and AP patterning defects. (F) Diagram illustrating the mean length-to-width ratio (ratio of the AP length of the adaxial domain to the embryo width at the level of the fifth somite) of control and *rpgrip1l* morphant embryos. In these morphants, all three expression domains are present and at the right place. However, all domains are wider along the DV axis and shorter along the AP axis in *rpgrip1l* morphants as compared with controls. The different AP landmarks of the neural plate: optic stalk, midbrain–hindbrain boundary, and rhombomeres 3 and 5 are also closer to each other. A widened and shorter embryo is indicative of CE defects and is a feature of the knock-down of PCP genes (Carreira-Barbosa et al., 2003) and of several ciliary genes (Ross et al., 2005; Gerdes et al., 2007). Together, these data show that early DV and AP patterning are not affected and that CE is perturbed upon Rpgrip1l depletion. Mhb, midbrain–hindbrain boundary; os, optic stalk; r, rhombomere; ad, adaxial domain; s, somites. (G and H) Lateral view of the floor plate of control (G) and Mo-Rpgrip1l–injected (H) Arl13bGFP transgenic embryos stained with antibodies specific for GFP and Ac-Tub and counterstained with DAPI. This transgenic line expresses an Arl13b-GFP fusion protein in all zebrafish embryonic cells and thereby permits to visualize the shaft of primary cilia, in which the small GTPase Arl13b trafficks (Borovina et al., 2010). Accumulation of Arl-13bGFP in the cilium of floor plate cells appears similar in control (G, $n = 12$) and *rpgrip1l* morphant (H, $n = 12$) embryos. (I–L) Control (I and K) and Mo-Rpgrip1l–injected (J and L) embryos were stained by immunofluorescence with antibodies specific for MKS1 (I and J), CEP290 (K and L), γ-Tub, and Ac-Tub. In zebrafish floor plate cells, Mks1 and Cep290 are present in granules along the cilium shaft. This localization is not significantly modified in *rpgrip1l* morphants. We counted the number of cilia presenting Mks1 or Cep290 staining. Mks1 granules were found on 79% of floor plate cilia in controls ($n = 71$ cells in 4 embryos) and on 75% of floor plate cilia in morpholino-injected embryos ($n = 80$ cells in 4 embryos). Cep290 granules were found on 48% of floor plate cilia in controls ($n = 72$ cells in 3 embryos) and on 60% of floor plate cilia in Mo-Rpgrip1l–injected embryos ($n = 74$ cells in 4 embryos). (M and N) *Centrin2-GFP* (*ctn2-GFP*) mRNA injected control (M, $n = 4$) and *rpgrip1l* morphant (N, $n = 4$) embryos were subjected to immunofluorescence for GFP (centrioles) and Ac-Tub (cilia). Neither defects in centriole engagement nor an abnormal number of centrioles per cell were detected (71 cells in 4 control embryos and 80 cells in 4 *rpgrip1l* morphant embryos were analyzed). (O–Q) *Ctn2GFP* RNA (15 pg) was co-injected with *mb-Cherry* (membrane-associated mCherry) RNA (22 pg) in control (O) or *rpgrip1l* morphant (P and Q) embryos in order to detect cell membranes and to correlate defects in asymmetric basal body positioning with eventual centriolar disengagement. The results show that centrioles are always in pairs and correctly assembled in close proximity to the apical membrane, even in cells that display anterior or medial basal bodies (P and Q). All pictures in G–Q are lateral views of the floor plate of flat-mounted 18-s embryos. All antibody stainings are indicated in the figure and color coded. Nuclei were stained with DAPI when indicated. Bars: (A, B, D, and E) 250 µm; (G–Q) 10 µm.

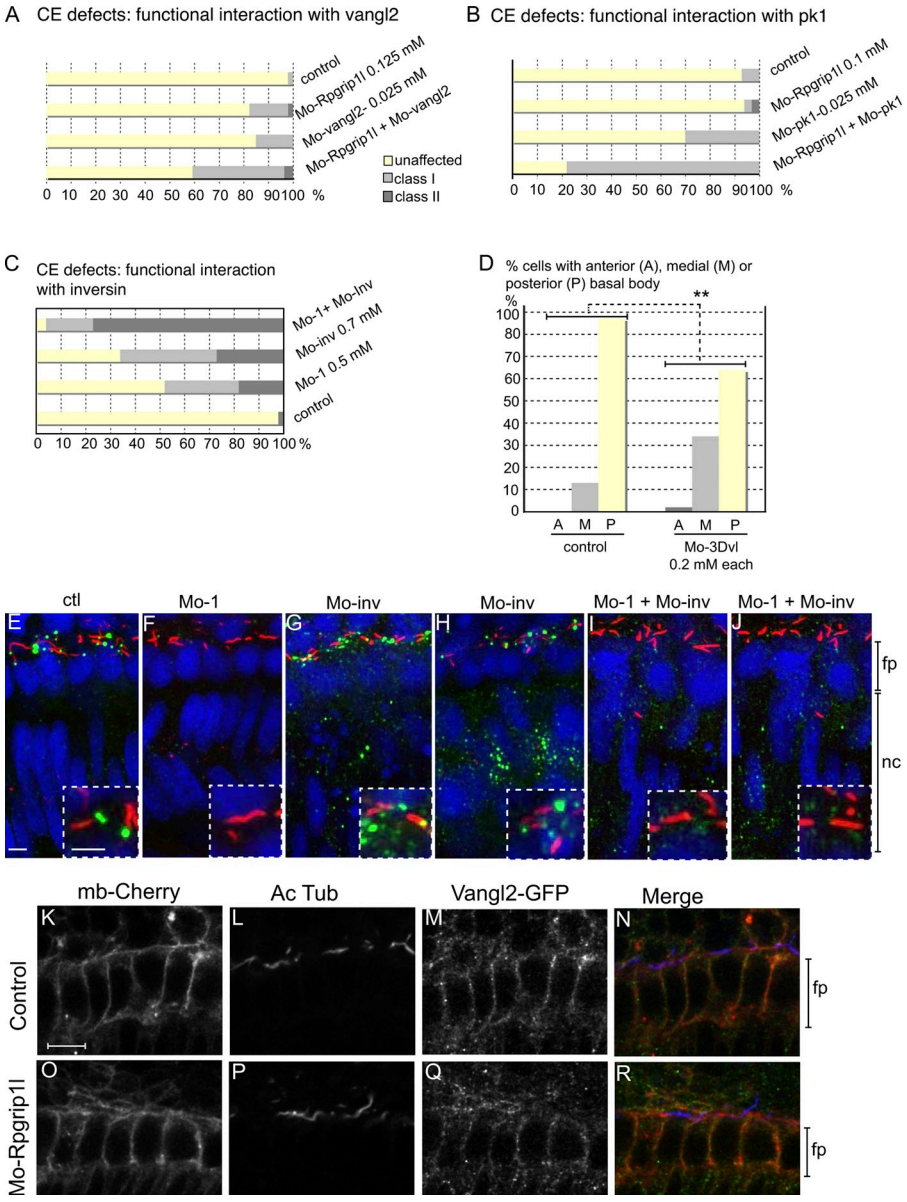


Figure S3. **Interaction of *rpgrip1l* with PCP genes and with *inversin*.** (A–C) Diagrams illustrating the functional interaction between *rpgrip1l* and the *vangl2* (A), *prickle1* (B), and *inv* (C) genes in axis elongation. Co-injection of Mo-Rpgrip1l with morpholinos specific for *vangl2* (A, Mo-vangl2), *prickle1* (B, Mo-pk1), or *inv* (C, Mo-inv) led to an enhancement of the morphant phenotype. For each lane, the injected morpholinos are indicated on the right. In A, $n = 25$ control, 21 Mo-Rpgrip1l–injected, 17 Mo-Vangl2–injected, and 22 co-injected embryos, from a representative experiment out of 4 repeats. In B, $n = 11$ control, 19 Mo-Rpgrip1l–injected, 22 Mo-Pk1–injected, and 20 co-injected embryos, from a representative experiment out of 4 repeats. In C, four independent experiments are represented. $n = 151$ control, 178 Mo-Rpgrip1l–injected, 126 Mo-inv–injected and 134 co-injected embryos. In A–C, the differences in the repartition in classes between batches of embryos injected with one morpholino only and the batch of co-injected embryos are significant ($\alpha < 0.001$, Khi2 test). (D) Diagram illustrating the percentage of floor plate cells with a basal body in posterior (P), medial (M), or anterior (A) position in 18-s stage embryos, either uninjected or injected with a mixture of morpholinos targeting each of the 3 zebrafish *dvl* genes (Mo3Dvl; 0.2 mM each). The diagram corresponds to a total of 5 control embryos (252 cells analyzed) and 5 Mo3Dvl-injected embryos (204 cells analyzed), from a single representative experiment out of 3 repeats. The double asterisk means that the differences are statistically significant (Khi2 test: $\alpha < 0.001$). This experiment shows that the posterior localization of basal bodies in floor plate cells depends on the concentration of functional Dvl proteins and suggests that the reduction in Dvl amounts in *rpgrip1l* morphants may be the cause of basal body localization defects. (E–J) Immunofluorescence with an anti-GFP antibody to reveal the GFP tagged Dsh protein and with an anti-acetylated α-tubulin antibody (Ac Tub) to label cilia in embryos injected with *DshGFP* RNA (10 pg/embryo) without morpholino (E) or with Mo-1 (F), Mo-inv (G and H), or both (I and J). In control embryos, DshGFP accumulated at the cilium base in notochord and floor plate cells (E). In embryos co-injected with Mo-Rpgrip1l and *DshGFP* RNA, DshGFP was severely reduced at the cilium base (F). Mo-inv–injected embryos showed increased Dsh-GFP levels in the cytoplasm as compared with controls, whereas the basal body pool appeared unaltered (G and H). In double morphants, the pool of dishevelled at the cilium base was severely reduced or absent, and the cytoplasmic pool was reduced compared with inversin morphants, but higher than in controls (I and J). Insets in E–J show higher magnifications in the floor plate region. These experiments show that Rpgrip1l and inversin interact positively for PCP and suggest that each protein acts preferentially on a specific cellular pool of dishevelled: inversin mainly destabilizes the cytoplasmic pool, whereas Rpgrip1l mainly stabilizes the basal body pool. Bars: (E–J and insets) 5 µm. (K–R) Immunofluorescence on control (K–N) and *rpgrip1l* morphant (O–R) embryos at the 14-s stage co-injected with *vangl2-GFP* (25 pg) and *mb-Cherry* (22 pg) mRNAs. Lateral view of a few floor plate cells of flat-mounted embryos are shown. The epitopes detected by the antibodies are indicated on the top of the picture. In the merge picture, cilia (Ac Tub) are blue, membranes (mCherry) are red, and Vangl2 (GFP) is green. The Vangl2-GFP protein is present in the membrane of floor plate cells without any obvious anterior or posterior enhancement, and no obvious modification of this pattern is observed in *rpgrip1l* morphants. However, an asymmetric accumulation of Vangl2 could be missed in these overexpression experiments. Bar: (K–R) 10 µm.

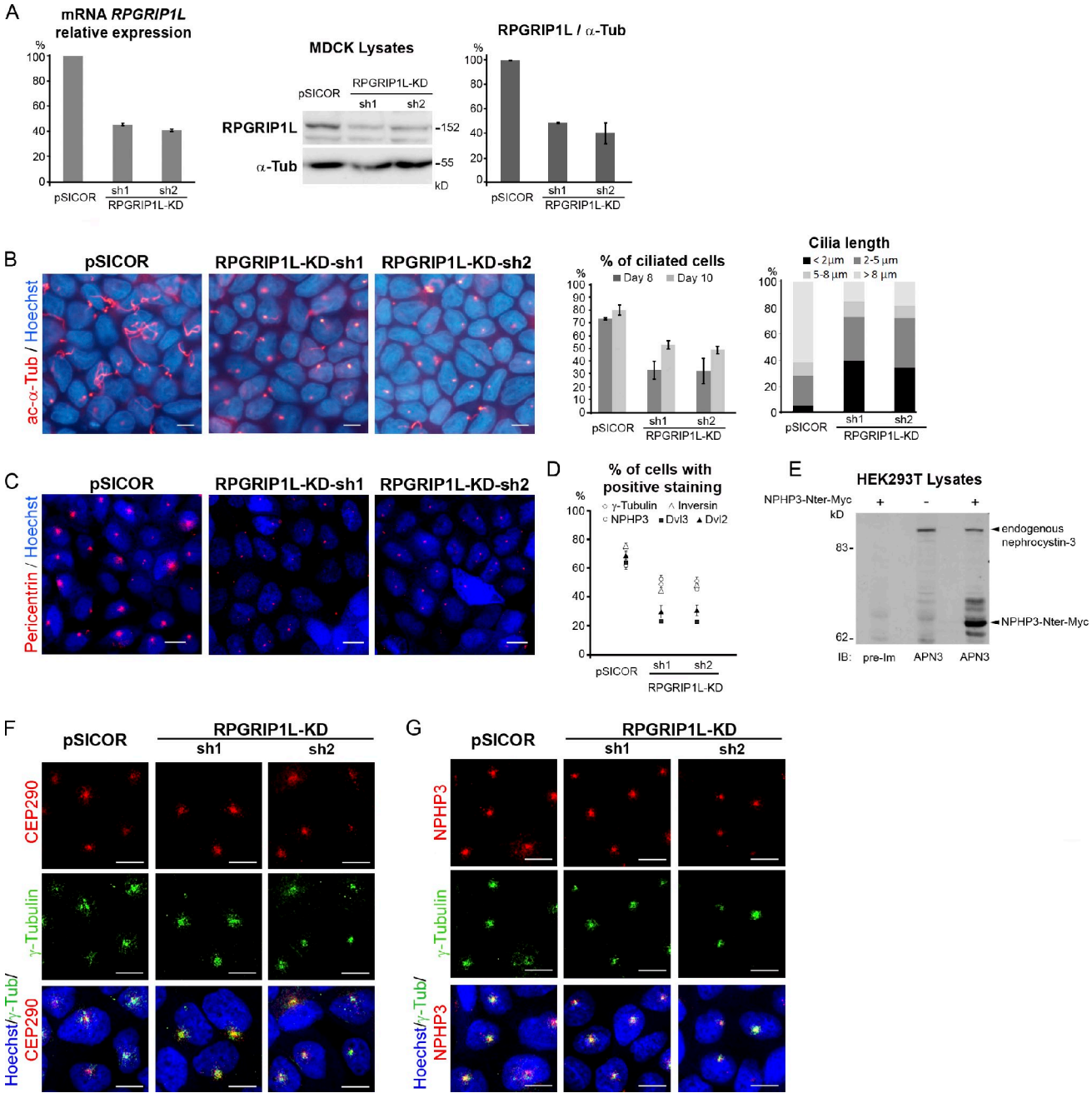


Figure S4. **Cilium and basal body integrity in MDCK cells upon RPGRIP1L depletion.** (A) Quantitative RT-PCR and Western blot analysis of the canine *RPGRIP1L* gene and protein product expression levels in polyclonal MDCK cell lines depleted for *RPGRIP1L* (RPGRIP1L-KD-sh1/sh2) and control cells (pSICOR). (B) Immunostaining of acetylated α-tubulin (ac-α-tub) performed on pSICOR and RPGRIP1L-KD cells after PFA fixation. The diagrams present the percentage of ciliated cells and cilium length in RPGRIP1L-KD versus control cells ($n$ = 1,500). (C) Pericentrin (red) staining after PFA/Pipes fixation was reduced in RPGRIP1L-depleted cells compared with control pSICOR cells, suggesting a partial loss of the pericentriolar material. (D) The percentage of cells exhibiting a γ-tubulin staining after PFA fixation was reduced in RPGRIP1L-KD-sh1/2 MDCK cell lines versus control pSICOR. While inversin or nephrocystin-3 were present in most of the γ-tubulin–positive RPGRIP1L-KD cells, Dvl2 or Dvl3 staining were lost in half of these cells (200–300 cells analyzed). (E) A specific affinity-purified rabbit antibody raised against the human nephrocystin-3 protein (aa 301–*577*; APN3) detected both the endogenous protein (132 kD) and the overexpressed truncated protein nephrocystin-3-Nter-Myc (aa 1–619; 72 kD) in HEK293T cells. No specific staining was observed with the preimmune serum (preIm). (F and G) Co-immunostaining of CEP290 (F) or nephrocystin-3 (G, red) with γ-tubulin (green) on RPGRIP1L-KD MDCK cells was not affected compared with control cells (pSICOR). Nuclei were stained with Hoechst. Bars, 10 µm.

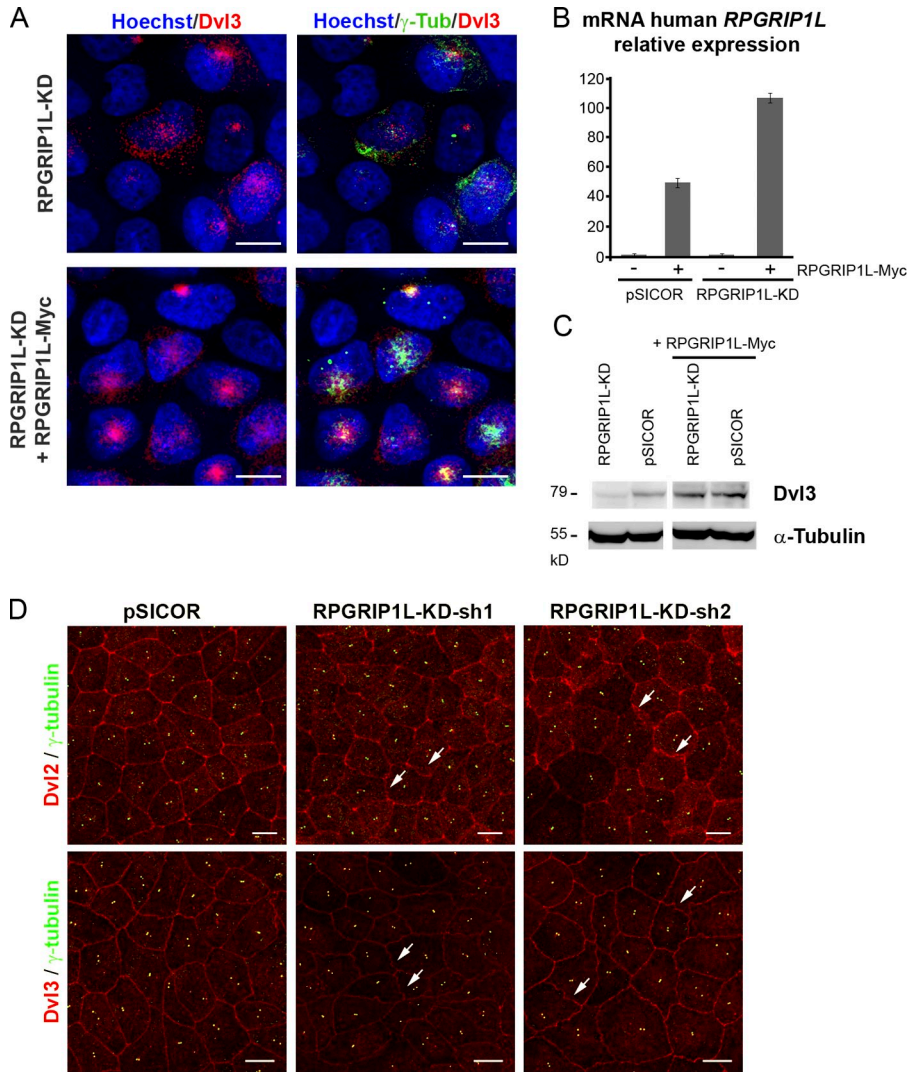


Figure S5. **RPGRIP1L depletion in MDCK cells: rescue and dishevelled localization at the membrane.** (A–C) Levels of Dvl3 proteins at the basal body are rescued by reexpression of RPGRIP1L. (A) Co-staining of Dvl3 (red) with γ-tubulin (green) after PFA fixation in RPGRIP1L-KD-sh1 MDCK cell lines with (bottom) or without (top) stable expression of RPGRIP1L-Myc demonstrates a rescue of Dvl3 accumulation at the centrosome/basal body in RPGRIP1L-reexpressing cells. (B) Quantitative RT-PCR analysis showing *RPGRIP1L-Myc* expression. (C) Western blot analysis reveals that expression of RPGRIP1L-Myc in RPGRIP1L-KD cells restores global Dvl3 protein levels. (D) Presence of Dvl2 and Dvl3 at the membrane of MDCK cells. Co-staining of Dvl2 or Dvl3 (red) with γ-tubulin (green) after methanol fixation in RPGRIP1L-KD-sh1/2 MDCK cell lines and control pSICOR. Methanol fixation permits the detection of dishevelled at the cell membrane and in faint dots at the basal body, but not in the pericentriolar material. Dvl2 and Dvl3 staining is present at the membrane in both control and RPGRIP1L-depleted cells, despite the wavy appearance of the cell junctions. A weaker staining was noted only for Dvl3 in RPGRIP1L-KD-sh1 cells. Bars, 10 µm.

## References


Borovina, A., S. Superina, D. Voskas, and B. Ciruna. 2010. Vangl2 directs the posterior tilting and asymmetric localization of motile primary cilia. *Nat. Cell Biol.* 12:407–412. http://dx.doi.org/10.1038/ncb2042

Carreira-Barbosa, F., M.L. Concha, M. Takeuchi, N. Ueno, S.W. Wilson, and M. Tada. 2003. Prickle 1 regulates cell movements during gastrulation and neuronal migration in zebrafish. *Development*. 130:4037–4046. http://dx.doi.org/10.1242/dev.00567

Gerdes, J.M., Y. Liu, N.A. Zaghloul, C.C. Leitch, S.S. Lawson, M. Kato, P.A. Beachy, P.L. Beales, G.N. DeMartino, S. Fisher, et al. 2007. Disruption of the basal body compromises proteasomal function and perturbs intracellular Wnt response. *Nat. Genet.* 39:1350–1360. http://dx.doi.org/10.1038/ng.2007.12

Ross, A.J., H. May-Simera, E.R. Eichers, M. Kai, J. Hill, D.J. Jagger, C.C. Leitch, J.P. Chapple, P.M. Munro, S. Fisher, et al. 2005. Disruption of Bardet-Biedl syndrome ciliary proteins perturbs planar cell polarity in vertebrates. *Nat. Genet.* 37:1135–1140. http://dx.doi.org/10.1038/ng1644